SPECTRAL AND SPATIAL DISTRIBUTION OF ACCELERATED PROTONS ON 11 MAY 2024

© 2025 S. V. Olemskoy*, I. I. Kovalev, M. V. Kravtsova***, and V. E. Sdobnov******

Institute of Solar-Terrestrial Physics of Siberian Branch of the Russian Academy of Sciences (ISTP SB RAS), Irkutsk, Russia

**e-mail*: osv@iszf.irk.ru

***e-mail*: ivankov@iszf.irk.ru

****e-mail*: rina@iszf.irk.ru

*****e-mail*: sdobnov@iszf.irk.ru

Received February 27, 2025

Revised April 10, 2025

Accepted May 22, 2025

Abstract. Ground-level enhancement (GLE) in cosmic ray intensity results from a short-term increase in the intensity of cosmic ray secondary particles revealed by ground-based detectors. The study of GLE provides information about acceleration mechanisms and particle propagation in the heliosphere. We investigated GLE74 (11 May 2024). It was the second GLE in 25 solar cycle related to a class 5.8 solar flare and a fast coronal mass ejection. The event was observed against the background of recovery of the Forbush effect. For our analysis, we used cosmic ray observational data from the worldwide network of neutron monitors that were processed using the method of global spectrographic survey. We also used data from GOES-16. Within the model of cosmic ray modulation by regular electromagnetic fields of the heliosphere, we determined the differential rigidity spectra of accelerated protons and their spatial distribution. The limiting rigidity of accelerated particles was estimated to be ~5–6 GV. We conducted a brief analysis of the cosmic ray spectra and anisotropy obtained during the GLE74 event comparing it to similar events that have been previously analyzed.

Keywords: *cosmic rays, ground level enhancement, rigidity spectrum, anisotropy*

DOI: 10.31857/S00167940250502e9

1. INTRODUCTION

Solar flares are known to generate high energy particles in the range from~ 1 MeV to ≥ 20 GeV (for protons). The appearance of solar cosmic rays (SCR) in interplanetary space, after explosive processes on the Sun (flares and/or coronal mass ejections (CMEs)), registered in the form of increasing particle fluxes, mainly on spacecraft (SC), is commonly referred to as solar proton events

(SPEs) (in the English-language literature - *Solar Particle Event* - SPE) [Miroshnichenko, 1973]. Such events belong to potentially dangerous manifestations of solar activity, they lead to an increase in the radiation level in the Earth orbit, deteriorate the work of radio navigation and can be harbingers of geomagnetic storms. Information about SPS (data on solar events with proton generation, energy spectra, etc.) is systematized into catalogs that are in demand by researchers (e.g., [Logachev et al., 2022]). The definition of the PCA is concretized. Thus, for events with non-relativistic particles the term PCA is applied, and for events with relativistic solar protons - GLE (*Ground Level Enhancement*) - ground-level increases of SCR [Oh et al., 2010; Miroshnichenko, 2014]. An updated definition of GLE is given in [Poluianov et al., 2017]. GLE events are recorded by ground-based detectors (neutron monitors (NMs), ground-based and underground muon telescopes, etc.). However, NMs remain one of the main instruments for making, with high accuracy, continuous measurements of the CL intensity at the Earth's surface. There are about 50 active NMs in the world network (https://nmdb.eu).

GLEs are rare events. From 1942 through December 2024, only 76 events have been recorded. The last GLE76 was registered on November 21, 2024 (https://gle.oulu.fi). In the previous, 24th solar cycle, there were only two such events: GLE71 (17.05.2012) and GLE72 (10.09.2017).

In this paper, we study the GLE registered on May 11, 2024. In the database (https://gle.oulu.fi), the event under study is assigned the number 74. This is the second GLE that occurred in the 25th solar cycle (at the time of writing, 4 events have been registered).

The source of GLE74 was a X5.8-class solar flare that began on May 11 at 01:10 UT (coordinates 17° S, 47° W) (https://kauai.ccmc.gsfc.nasa.gov/DONKI/). It generated a halo CME with a linear velocity of 1614 km/s (https://cdaw.gsfc.nasa.gov/CME_list/). The flare occurred in the extremely active region (AR) 13664, whose numerous energy releases since May 7, included a series of flares, 12 of which were of spectral class X, and were accompanied by a series of high-speed CMEs (https://www.solarmonitor.org; https://cdaw.gsfc.nasa.gov/CME_list/) [Hayakawa et al., 2024]. On May 10, the CMEs reached Earth and led to the most powerful geomagnetic storm in the past 20 years ($Kr = 9$; $Dst = -412$ nTL) [Spogli et al., 2024]. The modulus and *Bz component of* the interplanetary magnetic field (IMF) reached values of about 74 and -50 nTL, respectively (https://omniweb.gsfc.nasa.gov/ow.html). During the geomagnetic storm, the Forbush effect was observed in the CL [Mishev et al., 2024]. The amplitude of the decrease of CL intensity relative to mean daily CL intensity for May 8 at Oulu station (R_c= 0.72 GW) reached ~– 12%, in Irkutsk (R_c= 3.13 GW) - ~– 9%. The threshold rigidities of geomagnetic clipping (R_c) are given relative to the epoch of 2020 (https://tools.izmiran.ru/cutoff/).

At the background of the Forbush effect recovery on May 11 at 02:05 UT the increase of the count rate was recorded by the world network of NM stations. In particular, the amplitude of the effect at the high-latitudinal stations South Pole (R_c= 0.148 GW) and Oulu (R_c= 0.72 GW) comprised 8.7 % and 5.8 %, respectively, at mid-latitude station Irkutsk (R_c= 3.13 GV) - 4.5 % and at low-latitude stations Rome ($R_{(c)}$= 6.11 GV) and Alma-Ata (R_c = 5.87 GV) - 4.6 % and 4.8 %, respectively. The GOES spacecraft at this time registered an increasing flux of solar protons with energies above 100 MeV, which exceeded 1 pfu at 02:10 UT (https://kauai.ccmc.gsfc.nasa.gov/DONKI/).

The aim of this work is to obtain hardness spectra and CL anisotropy over a wide energy range during the GLE74 period. Such information will be useful in assessing the radiation situation in near-Earth space and in developing models of SCL propagation in the heliosphere.

2. DATA AND METHOD

Observations of the world network of NM stations (34 NMs) with a temporal resolution of 5 min (https://gle.oulu.fi; https://nmdb.eu) were used for the analysis. The modulation amplitudes were counted from the average NM count rate at each station of the world network for the time interval from 23:00 UT on May 10 to 01:00 UT on May 11.

The analysis was carried out using the spectrographic global survey (GGS) method [Dvornikov et al., 1997; Kovalev et al., 2022]. The method makes it possible to determine the orientation of the IMF, variation spectra and pitch-angle anisotropy of primary CLs, as well as the change in the planetary stiffness system of geomagnetic clipping and, using the data of observations of unstable charged components uncorrected for the temperature effect, the mean mass temperature of the atmosphere at the points where such observations are carried out.

For calculations of the differential stiffness spectra of primary CLs, we used the expression obtained in the framework of the model of CL modulation by regular heliospheric electromagnetic fields and data from the GOES-16 satellite (differential proton fluxes with effective energies (stiffnesses) of 2.7 MeV (7.1 MV), 8 MeV (12.3 MV), 16.5 MeV (177 MV), 27.9 MeV (230 MV), 52.7 MeV (319 MV), 134.9 MeV (521 MV), and 372.7 MeV (915 MV) recorded by the SGPS (*Solar and Galactic Proton Sensor*) instrument (https://data.ngdc.noaa.gov/). According to the data description (https://data.ngdc.noaa.gov/), the effective energies are the geometric mean of the energy ranges of proton registration in the instrument channels. The energy (hardness) ranges of proton registration on the GOES-16 spacecraft are 2.3-3.3 MeV (66-78.8 MV), 5.8-11.0 MeV (104-144 MV), 11.6-23.3 MeV (148-210 MV), 23.9-32.6 MeV (213-249 MV), 40.7-68.2 MeV (279-364 MV), 123-148 MeV (496-547 MV), 267-390 MeV (756-940 MV).

The expression to describe the CL stiffness spectrum is [Dvornikov et al., 2013]

$$J(R) = C \frac{\left(\varepsilon^2 - \varepsilon_0^2\right)^{3/2}}{\varepsilon[(\varepsilon + \Delta\varepsilon)^2 - \varepsilon_0^2]} \left(\frac{\varepsilon + \Delta\varepsilon}{T_0 + \varepsilon_0}\right)^{-\gamma},$$

where ε is the total energy of particles with stiffness R, $\varepsilon_0$is the rest energy, $T_0$is the kinetic energy at which the CL intensity of the corresponding stiffness is equal to C, γ is the spectral index of the galactic CL spectrum, Δε is the change in the total energy of particles in the heliospheric electromagnetic fields.

The data presented in the catalogs (https://kauai.ccmc.gsfc.nasa.gov/DONKI; https://www.solarmonitor.org; https://cdaw.gsfc.nasa.gov; https://omniweb.gsfc.nasa.gov) were used to describe solar activity, MMP, and NE.

3. RESULTS AND DISCUSSION

Fig. 1 shows the values of the MMP modulus and *Bz*-component of the MMP, NE velocity, longitude and latitude of the MMP orientation, variations of the isotropic component of the intensity of primary CLs with stiffnesses of 2 and 4 GW, amplitudes of the first $A_1$and second A_2harmonics of the pitch-angle distribution of CLs with stiffness of 4 GW for the period May 10-11, 2024.

Fig. 1.

A series of consecutive high-speed CMEs created an interplanetary perturbation, during which on May 10, against the background of a high-speed NE flow (velocity over 700 km/s) (Fig. *1c*), we observed a sharp increase in the MMP modulus to ~70 nTL (Fig. *1a*), and the value of the southern *Bz* component of the MMP was ~ -40 nTL (Fig. *1b*).

In Figs. *1d* and *1c*, a satisfactory agreement between the MMP orientation angles obtained by the GHS method and the spacecraft data can be seen.

The calculated increase in the particle intensity (Fig. *1e*) coincides with the fastest increase in the intensity of the neutron component of the secondary CLs at the NM South Pole (R_c= 0.148 GV). Thus, for particles with a stiffness of 2 GW, the largest increase in the particle flux occurred at 02:55-03:00 UT, and for particles with a stiffness of 4 GW - at 02:45-02:55 UT.

At some moments, an increase in the amplitude of $A_1$was observed (Fig. *1j*), which is an indicator of the Earth's passage through the MMP structures with increased field strength (Fig. *1a*): before GLE74, during the time interval from 00:15 to 01:45 UT, the amplitude of A_1did not exceed 8%, after the event - ~ 25%.40 min before GLE74, at 02:15 UT, the amplitude of A_2increased to 8% (Fig. *1z*).According to [Dvornikov et al., 2013] the increase in the amplitude of the second harmonic of the CL pitch-angle anisotropy indicates that at this time the Earth was inside the CME with a loop-like structure of the MMP.

Fig. 2.

Calculated differential stiffness spectra of protons in Earth's orbit at individual GLE74 time points are presented in Fig. 2. It can be seen from Fig. *2a* that the calculated differential stiffness spectra of protons agree well with the experimental data obtained on the GOES-16 spacecraft and the world network of CL stations.

The spectra of accelerated particles in Fig. *2b* are obtained by subtracting the background spectrum from the spectra at specific moments of time. The maximum hardness of the accelerated particles is ~ 5-6 GV.

Fig. 3.

In Fig. 3 shows the spatial distribution of particles with a stiffness of 2 GV in the solar-ecliptic geocentric coordinate system (GSE) for different GLE74 time moments. From Fig. 3, we can see that a bidirectional anisotropy is observed at the beginning of the event and at the time of maximum increase. At 02:30 UT, the enhanced CL fluxes come from the directions $\lambda = -15°$, $\Psi = 120°$ and $\lambda = 15°$, $\Psi = 300°$, while at 02:55 UT they come from the directions $\lambda = -15°$, $\Psi = 75°$ and $\lambda = 0°$, $\Psi = 270°$. At a subsequent time point (at 04:10 UT), unidirectional anisotropy is observed.

Table 1.

For comparative analysis we chose, analyzed earlier, GLE72 and GLE73 [Kravtsova & Sdobnov, 2021; Kovalev et al., 2025], which are identical to GLE74 not only qualitatively but also quantitatively (see Table 1). The first two columns of the table give the number of GLE and its date (day, month, year). The next two columns give the characteristics of the associated GLE flare: the X-ray and optical score, and the coordinates of the flare. Further are presented: the accompanying CME and its velocity; the magnitude of the maximum increase in the NM count rate; and the presence of the Forbush effect, against which the GLE was observed. The last two columns show the energy of accelerated SCRs and the presence of the second harmonic of pitch-angle anisotropy in the particle distribution.

Table 1 shows that some common features are evident between GLE72, 73, and 74: first, all GLE flares belong to class X, have significant power (the weakest of them served as a source for GLE73), and are located in the southern hemisphere of the Sun west of the central meridian. The W15-W90 zone contains more than 70% of all GLE flares [Belov et al., 2010]; second, the flares were accompanied by high-velocity halo CMEs; third, the maximum increase in the NM count rate was recorded at the South Pole station; fourth, they are characterized by relatively high values of accelerated SCRs and bidirectional anisotropy in the particle distribution; fifth, GLEs were observed against the background of the Forbush effect recovery (except for GLE73).

In general, the GLE74 event is more similar to GLE72 (see Table 1). The essential difference between them is the location of the source. The flare that caused GLE74 was close to the normal Parker spiral, while the source of GLE72 was closer to the solar limb. However, it should be noted

that the ordinary Parker spiral, strictly speaking, applies only to the unperturbed MMP, while the compared GLEs were observed against a background of strong heliospheric perturbations. Both events are characterized by bidirectional CL anisotropy, indicating that the Earth is in a "magnetic loop" associated with the Sun - specifically, with the AO where the GLE source was located.

Fig. 4.

In Fig. 4 presents for comparison the differential hardness spectra of the Sun-accelerated protons during the maximum increase of the CL intensity for the selected GLEs. It can be seen that in the low stiffness region (up to 1 GV) the spectra for GLE73 and GLE74 are close, while a significant discrepancy is observed in the relativistic region. For the events GLE72 and GLE74 the situation is opposite. In this case, the largest divergence in the differential stiffness spectra is traced up to ~ 2 GW, and at larger stiffnesses the spectra for these events are close.

The shape of the obtained particle spectra in the events GLE72 and GLE74 is consistent with the mechanism of SCR acceleration proposed by Berezhko & Taneyev [2013], when the acceleration of protons occurs by shock waves generated by the CME, taking into account the generation of Alven waves by the accelerated particles.

The stiffness spectra of the accelerated particles that we calculated include a stepped section $N \sim R^{(-)\gamma}$ up to 1 GV with exponentγ = 4.06 for GLE72 andγ = 4.96 for GLE74, ending with an exponential tail.

4. CONCLUSIONS

In the course of this study, differential stiffness spectra and spatial distribution of primary particles in the Earth's orbit were obtained on the basis of CL observations at the world network of CL stations and GOES-16 spacecraft. The maximum stiffness of accelerated protons was estimated at~ 5-6 GW. At the time of GLE74, the Earth was in the loop-like structure of the MMP. The differential proton stiffness spectrum for GLE74 in the stiffness range up to 1 GV is close to the proton spectrum of GLE73, and in the stiffness range above 2 GV to the proton spectrum of GLE72.

The proton acceleration in the GLE72 and GLE74 events is carried out by shock waves generated by the CME, taking into account the generation of Alven waves by accelerated particles.

ACKNOWLEDGEMENTS

The results were obtained on the equipment of the Angara Collective Use Center (http://ckp-rf.ru/ckp/3056/) and the Unique Scientific Facility "Russian National Ground-based Network of Cosmic Ray Stations (SCR Network)" (https://ckp-rf.ru/catalog/usu/433536/).

FUNDING

The work was carried out with the financial support of the Ministry of Science and Higher Education of the Russian Federation (Minobrnauka of Russia).

REFERENCES

1. *Belov A.V., Eroshenko E.A., Kryakunova O.N., Kurt V.G., Yanke V.G.* Terrestrial increases in solar cosmic rays in the last three cycles of solar activity // Geomagnetism and aeronomy. V. 50. No. 1. P. 23-36. 2010.

2. *Berezhko E.G., Taneev S.N.* Acceleration of solar cosmic rays by shock waves // Letters in V. 39, No. 6, P. 443-465, 2013. https://doi.org/10.7868/s0320010813060016

3. *Dvornikov V.M., Kravtsova M.V., Sdobnov V.E.* Diagnostics of electromagnetic characteristics of the interplanetary medium by effects in cosmic rays // Geomagnetism and aeronomy. V. 53. No. 4. P. 457-468. 2013. https://doi.org/10.7868/S001679401304007X

4. *Kravtsova M.V., Sdobnov V.E.* Terrestrial increase in cosmic ray intensity during the phase of decline of the 24th solar cycle: spectra and anisotropy // Izvestiya RAS. Ser. phys. V. 85. No. 8. P. 1194-1197. 2021. https://doi.org/10.31857/S0367676521080147

5. *Logachev Yu.I., Bazilevskaya G.A., Vlasova N.A. and others*. Catalog of solar proton events of the 24th cycle of solar activity (2009-2019). Moscow: MCD, 2022

6. *Miroshnichenko L.I.* Cosmic rays in interplanetary space. Moscow: Nauka Publ., 160 p. 1973

7. *The Russian national terrestrial network of cosmic ray stations.* 2025. https://ckp-rf.ru/catalog/usu/433536/

8. *The Angara Collective Use Center.* 2025. http://ckp-rf.ru/ckp/

9. *Cutoff2050 Geomagentic Calculator.* 2025. https://tools.izmiran.ru/cutoff/

10. *Dvornikov V.M., Sdobnov V.E.* Time variations of the cosmic ray distribution function during a solar event of September 29, 1989 // J. Geophys. Res. V. 102. A11. P. 24209–24219. 1997.

11. *GLE database.* 2025. https://gle.oulu.fi

12. *Hayakawa H., Ebihara Y., Mishev A., et al.* The Solar and Geomagnetic Storms in May 2024: A Flash Data Report // Astrophys. J. V. 979. № 1. P. 1–26. 2025. https://doi.org/10.3847/1538-4357/ad9335

13. *Kovalev I.I., Olemskoy S.V., Sdobnov V.E.* A proposal to extend the spectrographic global survey method // J. Atmos. Sol.-Terr. Phys. V. 235. P.105887–105894. 2022. https://doi.org/10.1016/j.jastp.2022.105887

14. *Kovalev I.I., Kravtsova M.V., Olemskoy S.V., Sdobnov V.E.* 2021 Oct 28 GLE73. First Event in Solar Activity Cycle 25: Spectra and Anisotropy // Bull. Russ. Acad. Sci.: Phys. (in press). 2025.

15. *Miroshnichenko L.I.* Solar Cosmic Rays: Fundamentals and Applications. Springer, 521 p. 2014.
16. *Mishev A., Larsen N., Asvestari E. et al.* Anisotropic Forbush decrease of 24 March 2024: First look // Adv. Space Res. V. 74. P. 4160–4172. 2024. https://doi.org/10.1016/j.asr.2024.08.027
17. *NASA/Goddard Space Flight Center*. 2025. https://omniweb.gsfc.nasa.gov/ow.html
18. *NOAA National Centers for Environmental Information*. 2025. https://data.ngdc.noaa.gov/
19. *NMDB: the Neutron Monitor Database*. 2025. https://www.nmdb.eu/
20. *Oh S.Y., Yi Y., Bieber J.W., Evenson P., and Kim Y.K.* Characteristics of solar proton events associated with ground level enhancements // J. Geophys. Res. V. 115. A10107. P. 1–14. 2010. https://doi.org/10.1029/2009JA015171
21. *Poluianov S.V., Usoskin I.G., Mishev A.L., et al.* GLE and sub-GLE redefinition in the light of high-altitude polar neutron monitors // Solar Phys. V. 292. № 11. P. 1–7. 2017. https://doi.org/10.1007/s11207-017-1202-4
22. *SOHO LASCO CME CATALOG*. 2025. https://cdaw.gsfc.nasa.gov/
23. *Solar Monitor*. 2025. http://www.solarmonitor.org/
24. *Space Weather Database of Notifications, Knowledge, Information* (*DONKI*). 2025. https://kauai.ccmc.gsfc.nasa.gov/DONKI/
25. *Spogli L., Alberti T., Bagiacchi P., et al.* The effects of the May 2024 Mother's Day superstorm over the Mediterranean sector: from data to public communication // Ann Geophys. V. 67. № 2. PA218. P. 1–31. 2024. https://doi.org/1044.01/ag-9117

Table 1. GLE events and associated flares and CMEs

GLE NO.	Date	Flash		CME V, km/s	Max %, station	Forbush effect	SCR acceleration, GW	A(2), %
		Score	Coordinates					
72	10.09. 2017	X8.2	09° S, 92° W	halo, 3136	8.0, South Pole	+	5-7	+
73	28.10. 2021	X1.0/2N	28° S, 01° W	halo, 1519	5.2, South Pole	-	3-5 two-stage acceleration	+
74	11.05. 2024	X5.8	17° S, 47° W	halo, 1614	8.7, South Pole	+	5-6	+

FIGURE CAPTIONS

Fig. 1. (*a*) - MMP modulus, (*b*) - *Bz-component of* MMP; (*c*) - NE velocity; (*d*, *e*) - longitude and latitude of MMP orientation (thin line - GHS calculation, thick line - spacecraft measurements); (*f*) - variations of primary CLs with stiffnesses of 2 GW (thin line) and 4 GW (thick line); (*g, h*) - amplitude of the first and second harmonics of pitch-angle anisotropy of CLs with stiffness of 4 GW. The vertical dashed line marks the onset of GLE74.

Fig. 2. Differential stiffness spectra of CLs: (*a*) - average spectrum two hours before the onset of GLE (dashed line), spectrum at the moment of GLE74 (solid line) and experimental data (icons); (*b*) - particles accelerated in the vicinity of the Sun at separate time moments of the development of GLE74: dashed line - at 02:30 UT, solid line - at 02:55 UT, dashed line - at 04:10 UT).

Fig. 3. Spatial distribution of primary particles with a stiffness of 2 GV in the GSE coordinate system at different moments of GLE74. The numbers on the curves indicate the levels of relative intensities of the primary CLs (in percent). The longitude (Ψ) is plotted on the abscissa axis and the angle latitude (λ) is plotted on the ordinate axis.

Fig. 4. Differential stiffness spectra of protons accelerated in the Sun's neighborhood during the maximum increase of the CL intensity for GLE: dashed line - GLE72 (10.09.2017 at 18:00 UT), dashed line - GLE73 (28.10.2021 at 17:05 UT), solid line - GLE74 (11.05.2024 at 02:55 UT).

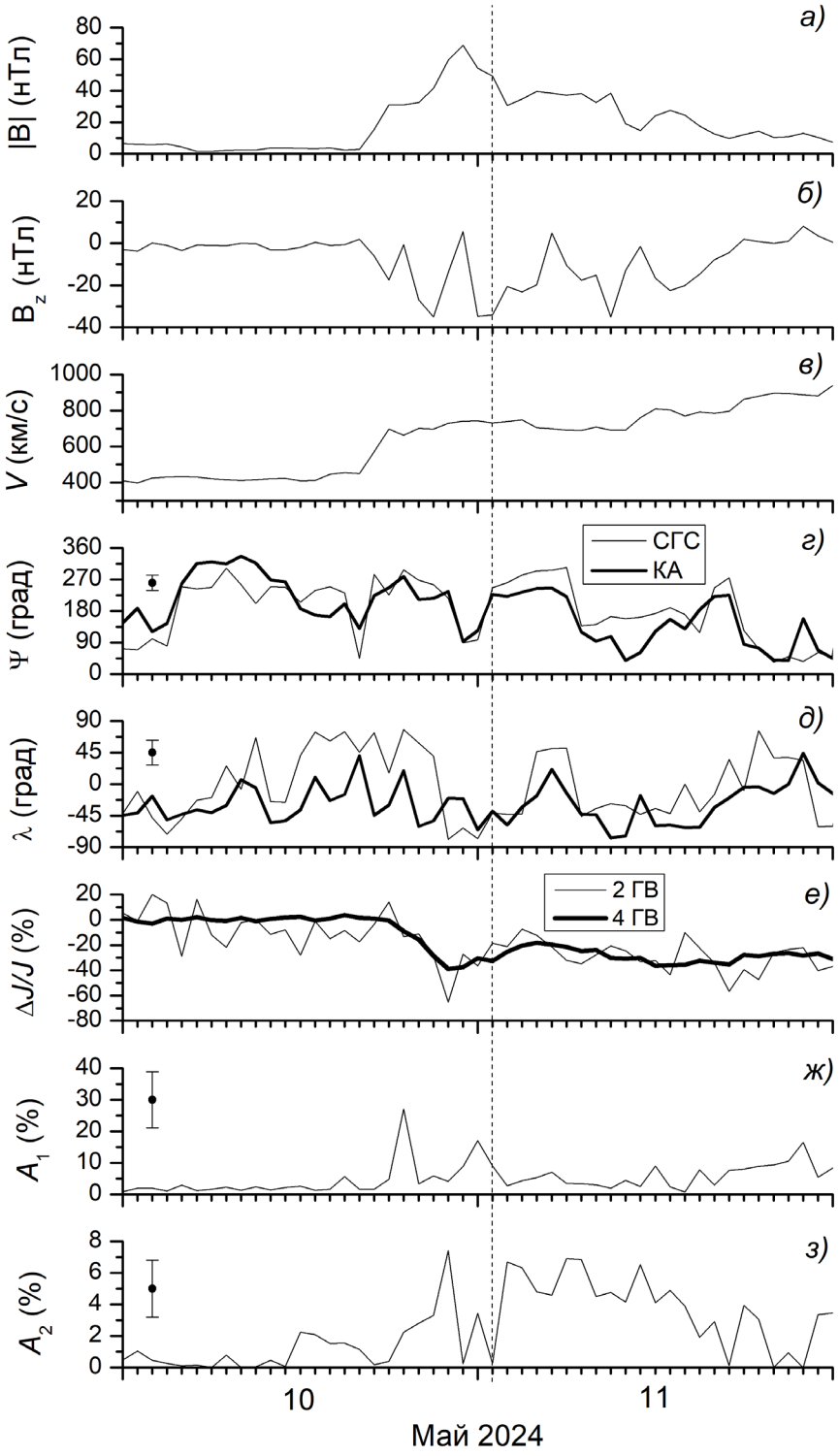
а)
|B| (нТл)
80
60
40
20
0
б)
B_z (нТл)
20
0
-20
-40
в)
V (км/с)
1000
800
600
400
г)
Ψ (град)
360
270
180
90
0
СГС
КА
д)
λ (град)
90
45
0
-45
-90
е)
ΔJ/J (%)
20
0
-20
-40
-60
-80
2 ГВ
4 ГВ
ж)
A_1 (%)
40
30
20
10
0
з)
A_2 (%)
8
6
4
2
0
10
11
Май 2024

Fig. 1.

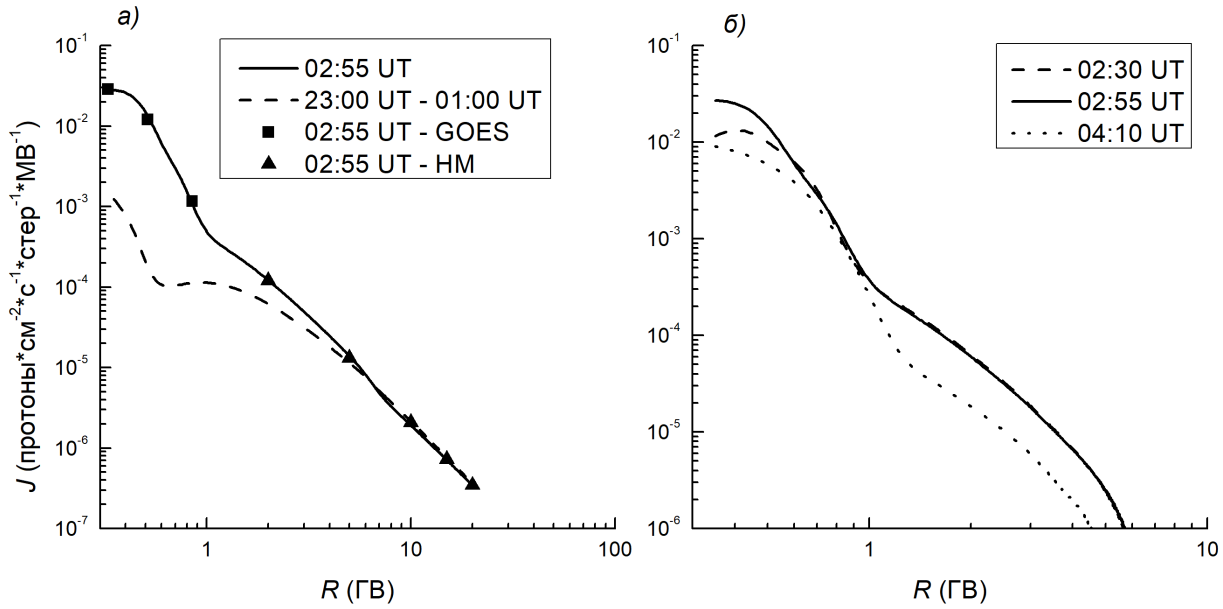
а)
б)
02:55 UT
23:00 UT - 01:00 UT
02:55 UT - GOES
02:55 UT - НМ
02:30 UT
02:55 UT
04:10 UT
J (протоны*см-2*с-1*стер-1*МВ-1)
R (ГВ)
R (ГВ)

Fig. 2.

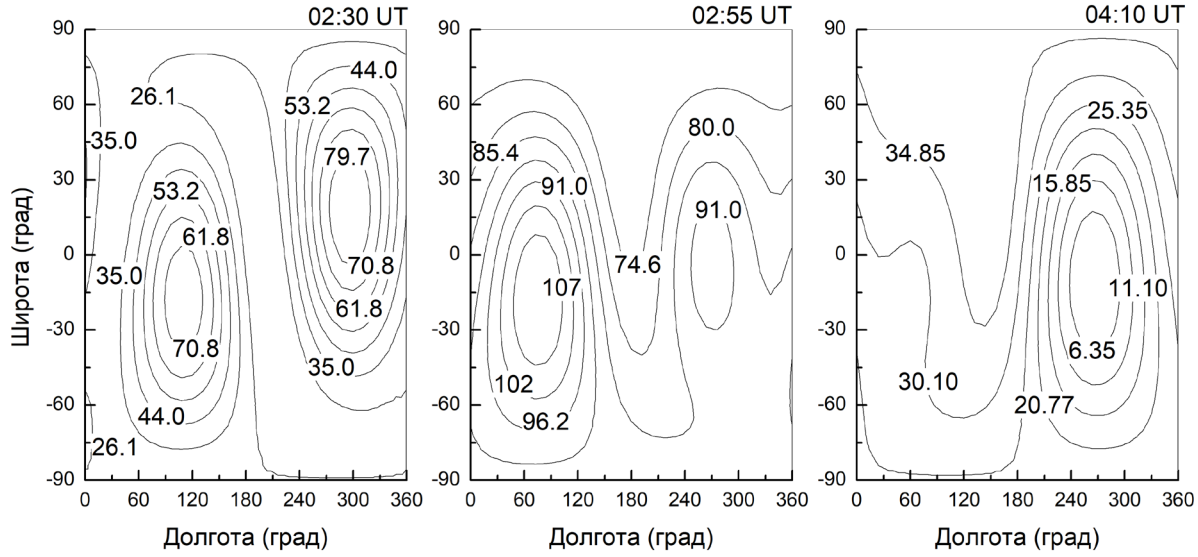
02:30 UT
02:55 UT
04:10 UT
Широта (град)
Долгота (град)
Долгота (град)
Долгота (град)
44.0
26.1
53.2
35.0
79.7
53.2
61.8
70.8
35.0
61.8
70.8
35.0
44.0
26.1
80.0
85.4
91.0
91.0
74.6
107
102
96.2
25.35
34.85
15.85
11.10
6.35
30.10
20.77

Fig. 3.

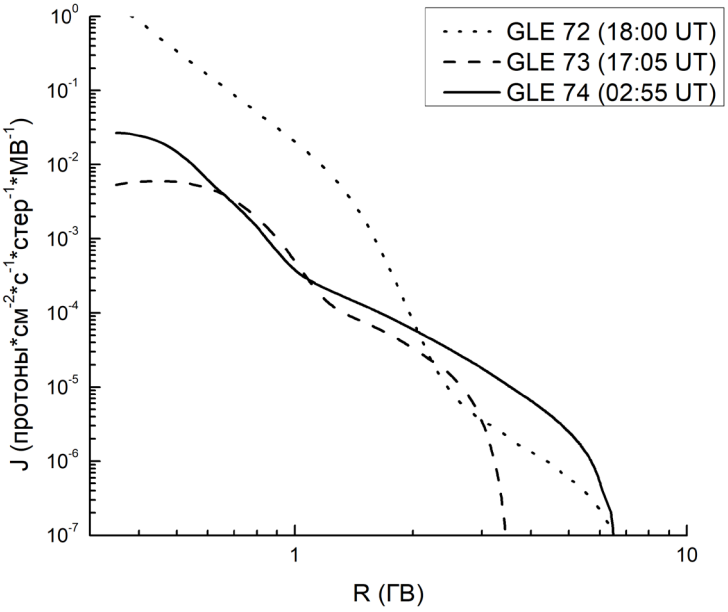
GLE 72 (18:00 UT)
GLE 73 (17:05 UT)
GLE 74 (02:55 UT)
J (протоны*см-2*с-1*стер-1*МВ-1)
R (ГВ)
10^0
10^-1
10^-2
10^-3
10^-4
10^-5
10^-6
10^-7
1
10

Fig. 4.